Recent Developments in Isogeometric Analysis with Solid Elements in LS-DYNA®

Liping Li
David Benson
Attila Nagy
Livermore Software Technology Corporation, Livermore, CA, USA

Mattia Montanari
Nik Petrinic
Department of Engineering Science, University of Oxford
Parks Road, OX1 3PJ, Oxford, UK

Stefan Hartmann
Dynamore GmbH, Stuttgart, Germany

Abstract

Isogeometric analysis (IGA), which uses the same geometry from CAD (computer-aided design) for numerical analysis, has been studied more and more in the past few years. The continuous development of IGA with shell and solid element has been added to LS-DYNA. Many of the standard analysis capabilities in LS-DYNA are now available for IGA such as explicit and implicit analysis. In this paper, we will provide updates on IGA: dynamics analysis using IGA solid, the implementation of user defined material including anisotropic material modeling and support for unstructured Spline capabilities through their Bézier extractions.

1. Introduction

IGA was introduced by Hughes [1] with the goal that the numerical analysis model is the same as the geometry from Computer Aided Design (CAD). Indeed, the finite element analysis (FEA), which is more and more widely used to solve various engineering problems, has a big limitation, that is, it can only approximate CAD geometries. This approximation limits the modeling fidelity, for example mesh generation, mesh refinement, sliding contact, flows about aerodynamic shapes, etc. Moreover, IGA adopts the same mathematical description for the geometry as in the CAD to replace the piecewise continuous Lagrangian polynomial which is the traditional interpolation function used in the FEM. At the same time, it can use the same framework of numerical method as in FEM.

There are however barriers to the applicability of IGA. Firstly, the behavior of IGA solid elements is not well understood. Secondly, modern CAD models are collections of surfaces and thus not suitable for analysis of solid structures. It is mainly for these reasons that, to date, IGA has limited industrial applications. The aim of the present work is to extend the applicability of IGA to solids modelled with complex material models. This paper is a part of that research effort and provide updates and guidelines to adopt IGA in industrial applications.

This paper is organized as follows:
In section 2, the basic ideas of Non-Uniform Rational B-Splines (NURBS) based IGA and Bézier-based IGA are introduced. Primary results of the IGA in LSDYNA will shown in section 3, including stress wave in solid rod, anisotropic material analysis and eigenvalue analysis on Bézier-based isogeometric models. Section 4 closes with some summary and an outlook.

2. Method

2.1 NURBS-based Isogeometric analysis

A NURBS is a piecewise polynomial splines that can efficiently represent complex geometries and conics (e.g. circles and ellipses). A NURBS curve can be represented as:

$$C(\xi) = \frac{\sum_{i=1}^{n} N_{i,p}(\xi) P_i w_i}{\sum_{i=1}^{n} N_{i,p}(\xi) w_i} = \sum_{i=1}^{n} R_{i,p}(\xi) P_i \tag{1}$$

where P_i is the control points, the index p is the order of the B-spline and n is the number of control points, w_i is the weight factor, and $R_{i,p}(\xi) = \frac{N_{i,p}(\xi) w_i}{\sum_{i=1}^{n} N_{i,p}(\xi) w_i}$.

The tensor product construct is used to define NURBS volumes (solid). Given a net of control points $\{P_{i,j,k}\}$, i=1,2,…n, j=1,2,…m, k=1,2,…,l, and three knot vector $U^1 = \{\xi_1, \xi_2, \dots, \xi_{n+p+1}\}$, $U^2 = \{\eta_1, \eta_2, \dots, \eta_{m+q+1}\}$ and $U^3 = \{\zeta_1, \zeta_2, \dots, \zeta_{l+r+1}\}$, the NURBS volume can be constructed as:

$$S(\xi,\eta,\zeta) = \frac{\sum_{i=1}^{n}\sum_{j=1}^{m}\sum_{k=1}^{l} N_{i,p}(\xi) N_{j,q}(\eta) N_{k,r}(\zeta) P_{i,j,k} w_{i,j,k}}{\sum_{i=1}^{n}\sum_{j=1}^{m}\sum_{k=1}^{l} N_{i,p}(\xi) N_{j,q}(\eta) N_{k,r}(\zeta) w_{i,j,k}} = \sum_{i=1}^{n}\sum_{j=1}^{m}\sum_{k=1}^{l} R_{ijk,pqr}(\xi,\eta,\zeta) P_{i,j,k} \tag{2}$$

where $w_{i,j,k}$ is the weight factor, and $R_{ijk,pqr}(\xi,\eta,\zeta) = \frac{N_{i,p}(\xi) N_{j,q}(\eta) N_{k,r}(\zeta) w_{i,j,k}}{\sum_{i=1}^{n}\sum_{j=1}^{m}\sum_{k=1}^{l} N_{i,p}(\xi) N_{j,q}(\eta)\, N_{k,r}(\zeta) w_{i,j,k}}$. An example of NURBS volume is shown in Fig. 1.

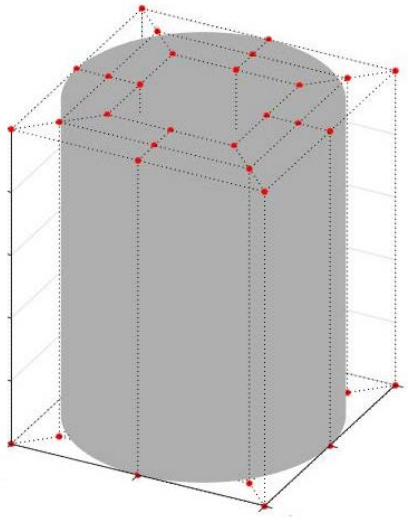

Figure 1 A NURBS volume example

In LS-DYNA, the keyword *ELEMENT_SOLID_NURBS are used to define the solid NURBS element, in which the information of knot vector, polynomial order and weight factors are defined. LS-DYNA will automatically calculate the basis functions and give the geometry of NURBS volume.

2.2 Bézier-based Isogeometric analysis

The Bézier extraction operator is a tool to decompose a set of NURBS or T-Spline basis functions to the Bernstein polynomials. It allows numerical integration of smooth functions to be performed on C^0 Bézier elements, giving a local representation of the basis functions.
A degree p Bézier curve is defined by a linear combination of p+1 Bernstein polynomial basis functions:

$$C(\xi) = \sum_{a=1}^{p+1} P_a B_{a,p}(\xi) = P^T B(\xi), \qquad \xi \in [0,1] \tag{3}$$

where P_a is the control points, $B_{a,p}$ is the Bernstein polynomial basis function.
The Bernstein polynomial basis function can be defined recursively as

$$B_{a,p}(\xi) = (1-\xi)B_{a,p-1}(\xi) + \xi B_{a-1,p-1}(\xi) \tag{4}$$

and

$$B_{1,0}(\xi) = 1 \tag{5}$$

$$B_{a,p}(\xi) = 0 \qquad if \;\; a < 1 \; or \; a > p+1 \tag{6}$$

From Bernstein polynomial basis function, it is easy to get NURBS basis function by:

$$N(\xi) = CB(\xi) \tag{7}$$

where C is the Bézier exaction operator. An example of how N and B basis functions look like is shown in Fig. 2. More details can be found in [2].

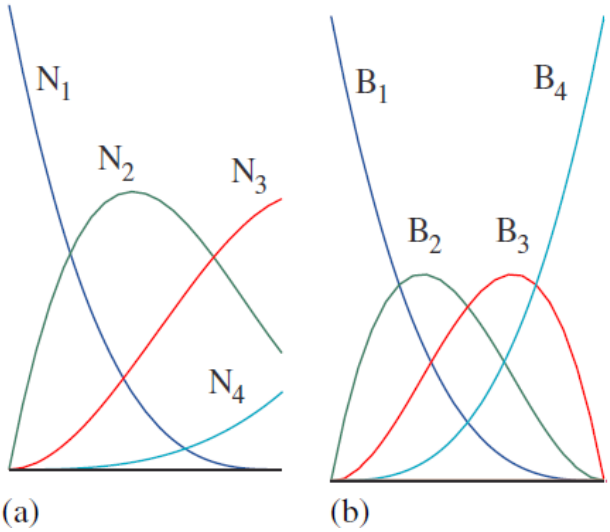

Figure 2 The basis functions over the knot span [0, 1[from (a) the NURBS basis and (b) the Bernstein basis.

In LS-DYNA, the keyword *INCLUDE_TRANSFORM is used to include the Bézier extraction operator, control points and weight information. LS-DYNA will automatically calculate the basis functions and return the geometry.

3. Analysis of IGA solid cases

3.1 Stress wave in solid rod

A uniaxial compression test specimen is loaded axially and the propagating stress wave is analyzed using IGA and FEA. The geometry of the specimen is a cylindrical solid rod of diameter d = 4.6 mm and length l = 8.0 mm. It is assumed elastic isotropic material, therefore MAT 001 is used, with Young's modulus E = 1.04 MPa, Poisson ratio ν= 0.3 and density ρ = 8.0e-9 m³/kg. A resultant force of 8310N is applied perpendicularly to one side of the rod, this is the input face. The load history is shown in Fig. 3, where the rising time t_r = 1/10 c and the striker time t_{st} = 9/10 c for a speed wave $c = \sqrt{\frac{E}{\rho}}$.

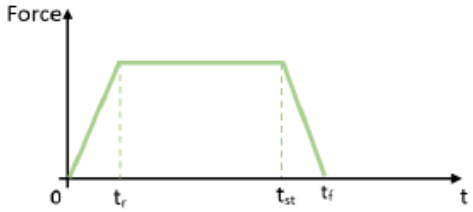

Figure 3 Axial pulse load history.

The solid rod is described using two analysis elements: hexahedral finite elements (ELEMENT SOLID) and a single NURBS patch (ELEMENT SOLID NURBS PATCH). Two examples of FEA and IGA are illustrated in Fig. 4.

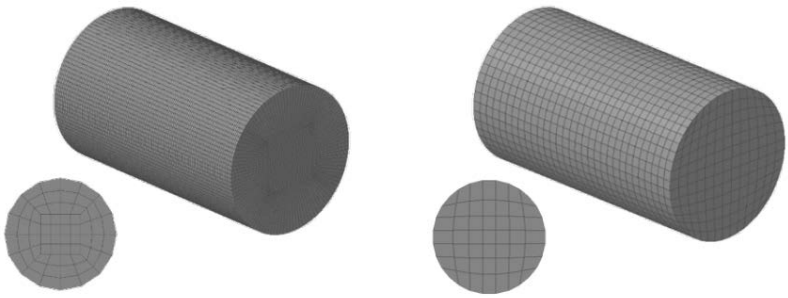

Figure 4 Spatial discretization of solid rod with FEA (a) and IGA (b)

Two levels of refinement are studied for both element types. A coarse FEA mesh is built with NC = NA =80, and a finer one with NC = NA = 110. The tri-variate NURBS patches are defined by mapping the parametric direction t to the axial direction, and r, s to the cross section. A coarse patch is defined by 20 intervals between the extrema of knot vector Ξ_T and 6 intervals for Ξ_R, Ξ_S, and polynomial orders p_T = 4 and p_R,p_S = 2. This is then refined to obtain a finer patch by doubling the internals for each knot vector, and p-refining of two orders each parametric direction.

For each one of the four FEA and IGA meshes, the tests are repeated using 1, 4 and 8 cores. This section compares the performance and the Von Mises stress obtained with FEA and IGA. The CPU time for each simulation is shown in Fig. 5(a). As expected, the coarse FEA mesh runs faster, while the finer IGA mesh results double as expensive. However, by looking at the CPU time for the other two meshes, IGA seems to scale better than FEA. This is confirmed by the relative gain in Fig. 5(b).

We can conclude that these (small) IGA models scale better on multiple cores than FEA. This is due to the more expensive element formulation of the former. Results are collected in Table 1.

The Von Mises stress predicted by FEA and IGA are compared. Fig. 6 and Fig. 7(a)-(b) show the stress distribution when the front of the travelling stress wave first reaches the middle of rod. Fig. 7(c)-(d) show stress isosurfaces when the front of the wave reaches the middle of the rod after bouncing back and travelling toward the input face. Despite the IGA mesh topology (see Fig. 4) introduces elements with poor aspect ratio, in all cases the stress distribution captured by IGA results significantly more homogeneous. More details of this study can be found in our former work [3].

Table 2 Profile results for the uniaxial pulse in solid rod test

Test ID	Method	P	Runtime 1 cores (min)	Runtime 4 cores (min)	Runtime 8 corse (min)
01	IGA	2,2,4	91	26	16
02	IGA	4,4,6	173	70	58
03	FEA	1	30	10	8
04	FEA	1	83	27	21

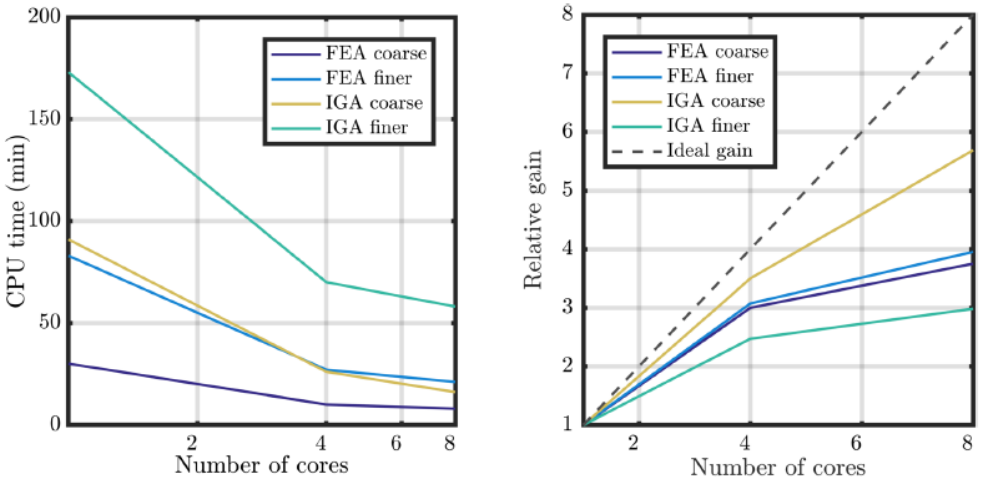

Figure 5 CPU time for solid rod test case. (a) Compares how CPU time of FEA and IGA scale for different levels of refinement as the number of cores increases. (b) Shows the relative gain for the same meshes.

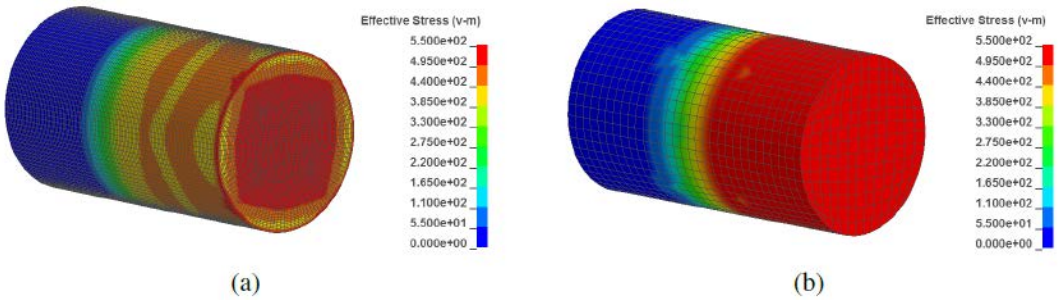

Figure 6 Compression of solid rod. Von Mises stress contour plots a $t=t_{st}/2$.

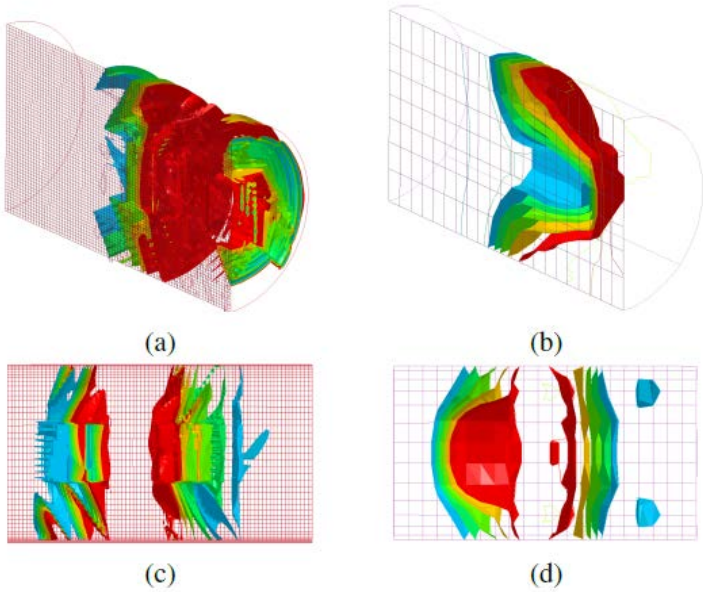

Figure 7 Von Mises stress distribution at t = t_{st}/2 for FEA (a) and IGA (b), and at t = t_{st}/0.5 for FEA (c) and IGA(d).

3.2 Anisotropic Material Analysis

We can now analyze anisotropic elastic and plastic material as well as isotropic material, such as *MAT_22,*MAT_033, *MAT_USER_DEFINED_MATERIAL_MODELS and etc.

The R-**value** (also called **Lankford value**, or plastic strain ratio) is a measure of the plastic anisotropy. If x and y are the coordinate directions in the plane of the model and z is the thickness direction, then the R-value is given by

$$R = \frac{\varepsilon_{xy}^{p}}{\varepsilon_{z}^{p}} \tag{8}$$

Where ϵ_{xy}^{p} is the plastic strain in-plane and ϵ_{z}^{p} is the plastic strain through-the-thickness.

In this study case, we selected a specimen shown in Fig. 8. The plasticity and anisotropic character is defined in *MAT_USER_DEFINED_MATERIAL_MODELS in Fig. 9. The Lankford values are set as R_{00}=0.6, R_{45}=0.7, R_{90}=0.8. And we compared two cases: the first one with vector a=[1 0 0], vector d=[0 1 0] which corresponds to R_{00}; the second with vector a=[0 1 0], vector d=[-1 0 0] which corresponds to R_{90}. The results are shown in Fig. 10 and show that the ratio of the in-plain strain and the through-the-thickness strain correspond to the input Lankford value.

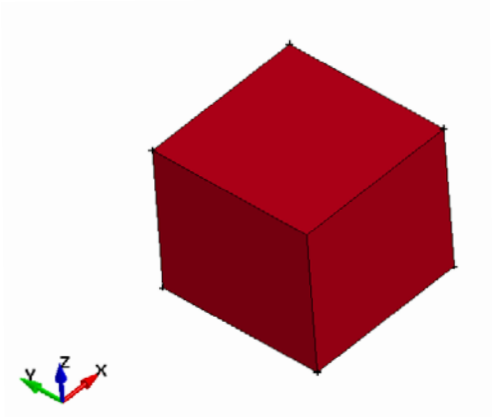

Figure 8 Anisotropic analysis model

```
*MAT_USER_DEFINED_MATERIAL_MODELS
$#     mid        ro        mt       lmc       nhv    iortho     ibulk        ig
     60002.79300E-9       283        40        13         1         3         4
$#   ivect     ifail    itherm    ihyper      ieos      lmca    unused    unused
         1         1         0         0         0         8
$#   aopt       mafc        xp        yp        zp        a1        a2        a3
       2.0       1.0       0.0       0.0       0.0       0.0       1.0       0.0
$#     v1        v2        v3        d1        d2        d3      beta     ievts
       0.0       0.0       0.0      -1.0       0.0       0.0       0.0         0
$#     p1        p2        p3        p4        p5        p6        p7        p8
  71000.0       0.3   69166.0   27307.0       0.0       0.0       0.0    6000.0
$#     p1        p2        p3        p4        p5        p6        p7        p8
       0.6       0.7       0.8       1.5       1.5       0.0       0.0       0.0
$#     p1        p2        p3        p4        p5        p6        p7        p8
       0.0       0.0       0.0       0.0       0.0       0.0       0.0       1.0
$#     p1        p2        p3        p4        p5        p6        p7        p8
       0.0       0.0       0.0       0.0       0.0       0.0       0.0       0.0
$#     p1        p2        p3        p4        p5        p6        p7        p8
       0.0       0.0       0.0       0.0       0.0       0.0       0.0       0.0
$#     p1        p2        p3        p4        p5        p6        p7        p8
       0.0       0.0       0.0       0.0       0.0       0.0       0.0       0.0
```

Figure 9 User defined material model

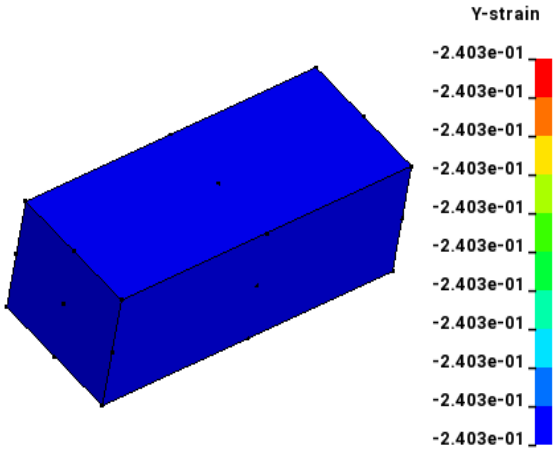

(a) Case I: y-strain

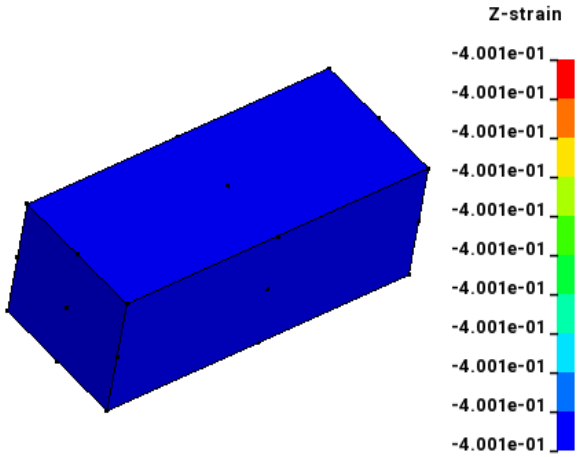

(b) Case I: z-strain

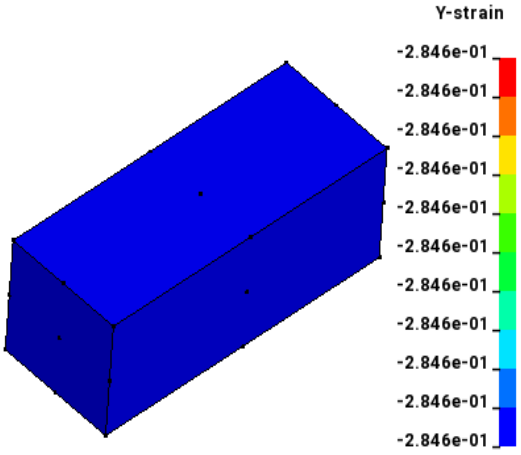

(c) Case II: y-strain

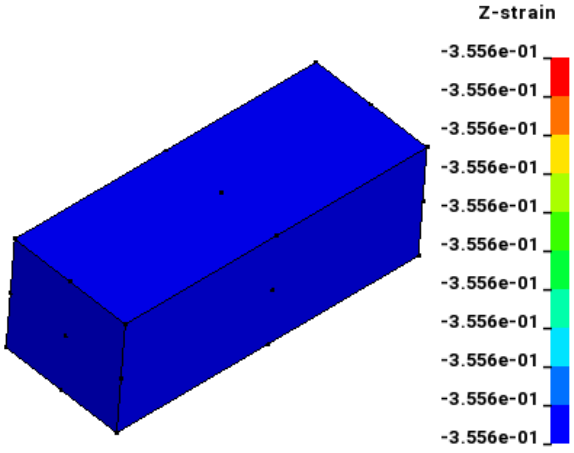

(d) Case II: z-strain

Figure 10 in-plain and through-the-thickness strain for case I and case II.
Case I: R=0.6; Case II:R=0.8.

3.3 Eigenvalue analysis with Bézier-based isogeometric model

The Bézier extraction operator allows numerical integration of smooth functions to be performed on C^0 Bézier elements. It gives a local representation of the basis functions, which make it possible to do local refinement on isogeometric element, while NURBS precludes local refinement because of its tensor product structure. For this reason, we started to implement Bézier-based isogeometric analysis in LS-DYNA.

Following we present three eigenvalue analyses of Bézier-based isogeometric models in LS-DYNA. The first model is a cross-hole (Fig. 11); the second one is a base model (Fig.12) and the third is a statue model (Fig. 13).

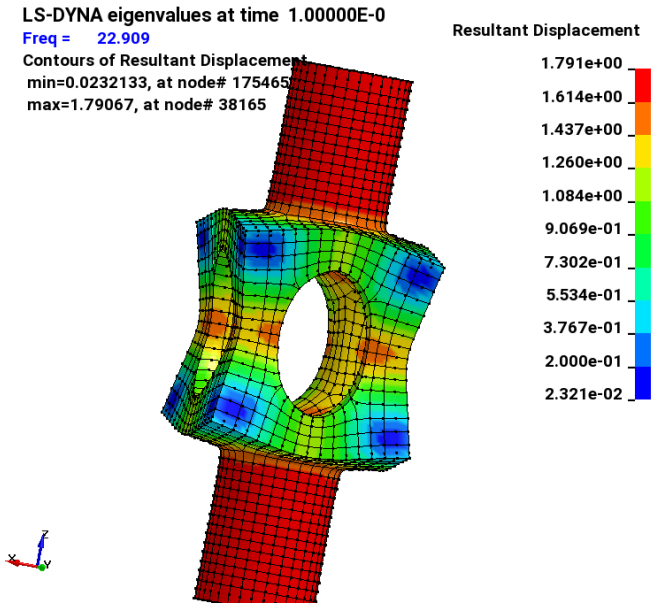

Figure 11 3rd eigenvalue result of the Cross-hole model

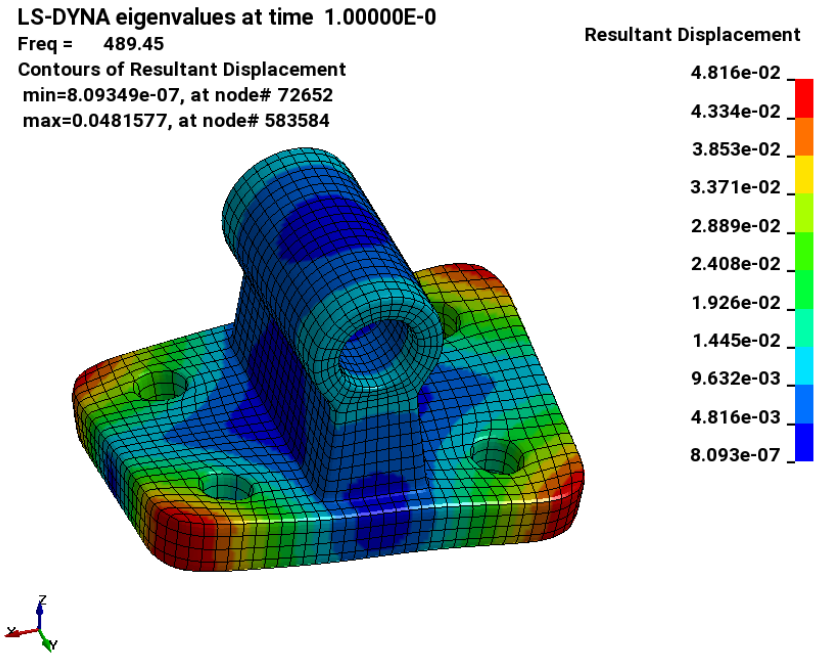

Figure 12 3rd eigenvalue result of the base model

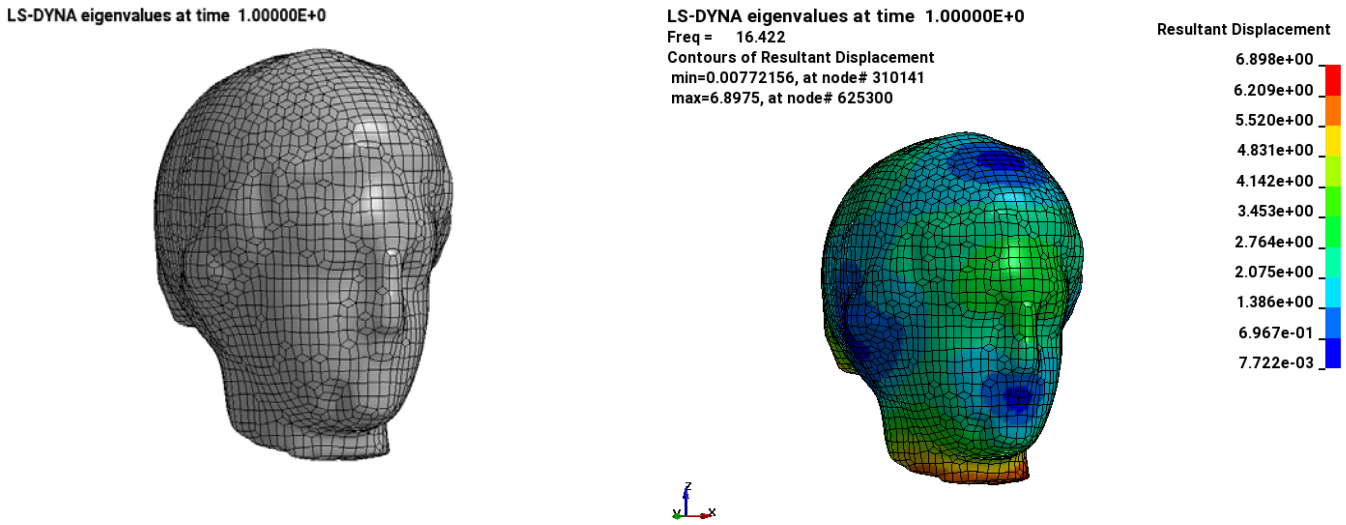

Figure 13 2nd eigenvalue result of the statue model

4. Conclusion

The basic ideas of IGA have been introduced along with a brief introduction of NURBS and Bézier extraction. Three study cases: stress wave in solid rod, anisotropic material analysis and eigenvalue analysis of Bézier-base isogeometric models are described to show LSDYNA capability to do various analysis on different isogeometric models. Future work will continue the development of IGA capabilities with in LS-DYNA.

References

[1] Hughes T J R, Cottrell J A, Bazilevs Y. Isogeometric analysis: CAD, finite elements, NURBS, exact geometry and mesh refinement. *Computer Methods in Applied Mechanics and Engineering*, 2005, 194(39-41):4135-4195

[2] Borden MJ, Scott MA, Evans JA, Hughes TJR. Isogeometric finite element data structures based on Bézier extraction of NURBS. *Int. J. Numer. Meth. Engng*, 2011, 87:15-47

[3] Montanari M, Li L, Petrinic N. Isogeometric models for impact analysis with LS-DYNA. 11th European LS-DYNA Conference 2017, Salzburg, Austria.